SLAC – PUB – 3512(REV.)
July 1985
M

Valence Band XPS-Study of Fe(100) at Finite Temperatures*

R.E. KIRBY, E. KISKER† F.K. KING, D. GURR, AND E.L. GARWIN

Stanford Linear Accelerator Center
Stanford University, Stanford, California, 94305

ABSTRACT

Measuring the valence band density of states (DOS) of Fe provides a stringent test of models of metallic ferromagnetism at finite temperatures. The density of states of Fe above the Curie temperature T_c, as obtained by self-consistent calculations in the disordered local moment (DLM) picture by Oguchi et al[1] and by Pindor et al[2] differs strongly from the T=0 DOS calculated by Moruzzi et al[3] between the Fermi energy and 2 eV binding energy, *i.e.* the relatively broad peak in the T=0 DOS around 1 eV binding energy is of much smaller amplitude in the $T>T_c$ DOS. This effect should be observable by valence band XPS on Fe as a 30% decrease of intensity at about 1 eV binding energy with a typical energy resolution of about 0.8 eV. We have measured the valence band XPS of Fe(100) at room temperature and temperatures above T_c. The predicted intensity decrease has not been observed.

Presented at the 30th Annual Conference on Magnetism
and Magnetic Materials, San Diego, CA, Nov. 27-30, 1984.

---

* Work supported by the Department of Energy, contract DE – AC03 – 76SF00515.
† present address: KFA, Institut fur Festkorperforschung, Postfach 1913, D-5170 Jülich, West Germany

1. Introduction

A long standing question is on the microscopic nature of the ferromagnetic to paramagnetic phase transition of the 3d-transition metals Fe, Co, and Ni. Although there is no doubt that long-range ferromagnetic order ceases to exist above T_c, it is a problem to reconcile this in a microscopic theory. There are several prominent models for explaining the loss of the magnitude of the spontaneous magnetization: the Stoner model[4,5], the disordered-local moment picture (DLM)[1,2] and a model based on disordering of some sort of magnetic clusters of size of 10–30 Å, which commonly is referred to as the fluctuating band picture[6]. Also, spin-spiral configurations have been used for modeling the magnetic structure above T_c.[7] The Stoner model assumes that the exchange splitting decreases proportionally to the spontaneous magnetization, with other thermal effects modeled by broadening the DOS.[5] In the DLM model, randomly oriented magnetic moments are assumed to exist on the lattice sites above T_c. Within the DLM framework, the electronic structure has been calculated recently self-consistently[2] and, it turned out that for Fe, the magnetic moment per site remains nearly constant up to T_c.

The electronic structure of Fe on which we will concentrate in this work has been previously studied by electron spectroscopic methods such as photoemission[8], spin-polarized photoemission[9], and x-ray photoelectron spectroscopy[10], and also, temperature effects have been studied.[11] Experimental angle-resolved photoemission measurements have been successfully compared with theoretical differential calculations (such as the bandstructure) at low temperatures with good agreement. However, comparison at elevated temperatures is complicated by the lack of electron- and spin-phonon coupling in the theory.

X-ray photoelectron spectroscopy (XPS) measures the density-of-states, rather than the band structure, as is known experimentally.[12] This has been explained as caused by a lack of electron-phonon coupling[13] or as being due to a loss of momentum conservation.[14] Therefore, the interpretation is easier since it is the

DOS which is measured at any temperature. Changes in the angular distribution which may occur in UPS due to electron-phonon coupling are absent in XPS, since even at room temperature, we effectively average already over the angular distribution.

Recently, the DOS of Fe above T_c has been calculated in two models, *i.e.* in the DLM picture,[1,2] and in the Stoner model[5] with broadening effects involved. We might expect that in a "cluster" model, the DOS should be the more similar to the low temperature DOS the larger the range of correlation is. Since the predicted effects on the DOS can be measured with XPS, we have performed this experiment for temperatures up to 1.03 T_c and we compare the data with the theoretical predications. Valence band UPS of Fe at elevated temperatures (but $<T_c$) has been measured previously,[9] but the conclusion was that no change is observed in the energy distribution curve (EDC) with increasing temperature.

2. Experiment

2.1 Sample Preparation

The α-Fe(100) sample was a .6 cm diameter $\times$ .02 cm thick disk which was polished mechanically with 0.5 μ diamond paste, degreased and chemically polished. The sample was cleaned in situ by repeated cycles of argon ion sputtering (1000 eV) and annealing (825–875 K). The sample was demagnetized prior to insertion into vacuum and by raising it above the Curie temperature (1043 K) *in vacuo* prior to the experimental data taken and presented here.

2.2 Vacuum System

Measurements were made in a baked ultrahigh vacuum ($P < 3 \times 10^{-10}$ torr) system pumped by a combination of ion, sublimation and, during heating to the Curie temperature, cryo pumps. The maximum pressure during the heating experiments was $< 2 \times 10^{-8}$ torr.

2.3 XPS, AES SPECTROMETER

The surface cleanliness of the sample was checked using AES and XPS. The analyzer was a Vacuum Generators Ltd. CLAM ESCA 3 unit incorporating a 150^o electrostatic spherical sector with a magnification one transfer lens at its input. The analyzer entrance and exit slits are variable. For this experiment two slit sizes were used, $2 \times 4\text{mm}^2$ and $4 \times 4\text{mm}^2$. The x-ray source was a Mg anode ($\text{K}\alpha_{1,2} = 1253.6$ eV) operated at 240 watts. The combined x-ray source-analyzer resolution (hereafter referred to as "the instrument resolution") was measured using the Pd Fermi edge (B.E. = 0) which gave 1 eV FWHM and 0.8 eV FWHM for the 4 and 2mm slits, respectively. The analyzer pass energy was constant at 20 eV. The angle of the source and analyzer to the sample surface normal was 18.5^o and 15^o, respectively.

AES measurements were made using the same analyzer and an electron gun operating at 4.9 KeV with a beam current density of $2 \times 10^{-3} A/m^2$ and a rastered beam current of 50 nA.

System control and data acquisition is under computer control (LSI 11 microcomputer). Data in pulse count form is collected from the analyzer channel-electron-multiplier via a pulse height amplifier and scaler and is stored on hard disk for later analysis. Data can be collected in both multipass (*e.g.* for AES analysis) or profile mode (*e.g.* Fe XPS valence band during temperature increase, as a function of time).

Data runs were made at room temperature during which the Fe XPS spectrum was measured in the range -1.9 to 120 eV(Fe 3s,3p) or -1.9 to 14 eV(Fe valence band) binding energy. Four valence band runs were made while heating the Fe to above the Curie temperature. After cleaning at room temperature, the AES background subtracted peak height ratio averages obtained in the energy distribution mode for impurity elements were: S(146 eV)/Fe(700) = 0.10, C(263)/Fe(700) = 0.05, N(375)/Fe(700) = 0.04. Roughly estimating the average contamination levels that these numbers represent (using a commercially avail-

able AES sensitivity listing)[15] gives: S/Fe = 0.03, C/Fe = 0.08 and N/Fe = 0.04. AES was also done on two of the heating runs while near the Curie temperature. There the only surface contaminant was S; the peak height ratios were S/Fe = 0.076 and 0.23. This would be, after sensitivity adjustment, S/Fe = 0.065 and 0.214. The heating data consistently gave the same shape and peak height results for the valence band of Fe independent of these residual S levels.

2.4 Heating and Temperature Measurement

For ease of handling, the Fe sample was mounted into a Nb disk sample holder with a closed back. The Fe surface was coplanar with the Nb surface.

The back of the Nb holder was heated by electron bombardment from an enclosed, bifilar-wound W filament. The Nb and surrounding surfaces were maintained at ground potential during the heating and the Fe crystal was heated by conduction from the Nb.

The Fe temperature was measured with an infrared pyrometer which was calibrated after the valence band data was taken by comparison to a chromel-alumel thermocouple, spot-welded directly to the Fe. The calibrated pyrometer readings were used to determine the Fe emissivity as a function of true temperature. The emissivity versus true Fe temperature data was fitted to a polynomial which was then used to obtain the Fe temperatures used in the valence band data.

During valence band data acquisition the Fe could not be viewed directly; however, the sample temperature was monitored using a W 5% Re – W 26% Re thermocouple which was spot-welded to the sample clip that held the Nb disk. The response of this thermocouple was calibrated prior to the actual data run by comparison to pyrometer readings of the directly viewed Fe surface.

To ensure that the current flowing in the heated filament was not producing a magnetic field effect, the current was run up quickly while the valence band spectrum was monitored and before the sample achieved a significant temperature rise (due to the lag between the heated rear surface of the Nb and the Fe). No

effect on the shape or intensity was observed. In addition an identical filament was set up external to the system and the magnetic field with current flowing was determined using a Hall effect gauss meter. At the maximum heating current used to achieve the highest sample temperature the field component at the Fe surface position is 0.18 gauss for the parallel and 0.93 gauss for the normal components. These measurements were made in the absence of ferromagnetic material.

To ensure that the proximity of the heated Fe was not untowardly affecting the analyzer, in one experiment the sample was heated to above T_c away from the analyzer and shifted to it for valence band measurement. No effect of sample temperature on the analyzer could be observed.

2.5 Data Analysis

The XPS analyzer accepted photoelectrons generated from a sample area somewhat larger than the Fe crystal, for both the 4 × 4 and 2 × 4mm^2 slits. The XPS spectrum of the Nb sample holder was measured from -1.9 to 120 eV B.E. at 295K and 1080K for each of the slit sizes and the Nb contribution has been removed from the data presented here. No change in the valence band of Nb was detected at these two temperatures and thus this procedure is believed to be valid. The Nb contribution to the peak signal intensity of the 2 and 4mm slits as a percentage of the Fe intensity was (prior to its removal) 28% and 40%, respectively. The areal signal contribution from -1.9 to 14.1 eV B.E. for the 2 and 4mm slits was 22% and 31%, respectively.

Smoothing of the data was accomplished using a spline smoothing technique. We used the I.M.S.L.[16] routine ISCCSU which is based on the algorithm given by Reinsch.[17] This method uses variational methods to find the smoothest function consistent with the data. The ISCCSU routine requires two variables, a global parameter S to control the amount of smoothing done and a vector of weights assigned to the data points. However, the values suggested by Reinsch were not suitable. Instead, we assigned equal weights to the data points and

determined the value of the global smoothing parameter by first smoothing the data using a B-spline[18] smooth and estimating the noise present. These values were then held constant for the smoothing of the data taken under similar experimental conditions.

3. Results

3.1 Room Temperature

Figure 1 is a room temperature (295 K) survey of Fe(100) up to 120eV binding energy. The shapes and peak ratios for the 3s and 3p states agree well with the work of Fadley and Shirley[10] for hydrogen-annealed Fe.

Figure 2 shows our measured valence band XPS for Fe at room temperature. An attempt was made to curve fit this experimental data using several approaches. These were: 1) convolution of the spin-summed T=0 DOS by Moruzzi et al[3] with the instrument resolution (see Section 2.3) where a Shirley background [19] is added to the result; 2) same as case number 1 except the spin-summed DOS of Ohnishi et al[20] (center layers only, explained below) is used; 3) same as case number 2 except one surface plus seven center layers; 4) same as case number 2 except two surface plus six center layers; 5) same as case number 1 with lifetime broadening and matrix element correction included.

We treat each of these cases in turn. When the fits are done, a constant background level due to bremsstrahlung processes is added to whatever background is present in the fit. This bremsstrahlung background level is equal to the count rate at BE < 0 and is assumed to be constant over the BE range of $\sim$16eV that the experimental data is taken.

1) Moruzzi et al[3] convolution:

Figure 3 shows the result of convolving the sum of the ferromagnetic spin-majority and minority T=0 DOS's of Moruzzi, Janak and Williams [3] with the

instrument resolution and adding a Shirley background[19]. The Shirley background models the inelastic-electron background signal by assuming that the background at a particular binding energy is proportional to the integrated intensity of unscattered electrons at lower binding (higher kinetic) energies with the proviso that the calculated background matches the experimental background outside the peak region.

The shape of the fit in Figure 3 is obviously rather poor. The peak locations are well reproduced at 1, 3 and 5eV. However, there seems to be a substantial broadening effect which has not been taken into account or, alternatively, the shape of the Moruzzi et al[3] DOS is incorrect.

2) Ohnishi et al[20] convolution, center layers only:

A recent T=0 ferromagnetic DOS calculation for Fe(100) by Ohnishi, Freeman and Weinert[20] includes, as a parameter, the variation of the ferromagnetic charge as a function of distance from the surface. The various layers are considered as surface or center (bulk) layers. The DOS, based on center layers only, should be similar to the Moruzzi et al[3] DOS considered above, although the different calculational methods used might be expected to yield minor disagreement between the two DOS's.

Figure 4 shows the result of convolving the spin-summed center-only DOS with the instrument resolution and adding the appropriate Shirley background. As in the Moruzzi et al fit of Figure 3, the peak positions are correct and, in addition, the ratio of the 1 to 3eV peak intensities is much improved. However, despite a difference in the DOS due to calculational method, there is still a significant amount of missing broadening and/or states evident above 2eV.

3) and 4) Ohnishi et al[20] convolution, mixture of surface and center layers:

In this convolution is included the effect of the reduced ferromagnetic surface charge used to calculate the DOS. Ohnishi et al[20] present DOS's for center layers and surface layers individually. The inelastic mean free path for our 1250eV

photoelectrons is about eight layers[21]. We have scaled and added together the surface and center layer DOS's to give the equivalent of a one surface-seven center layer (Figure 5) and a two surface-six center layer (Figure 6) convolution with the instrument resolution (with Shirley background added to each calculation). The result shows that, even with increased surface contribution, the agreement with experiment is still poor for E_B greater than 2eV. This suggests that the source of the broadening is not included in either of these DOS's.

5) Moruzzi et al[3] DOS with lifetime broadening:

Good agreement with experiment has been obtained by several workers[22–25] for various materials by including the effects of photohole lifetime broadening and matrix element modulation. The lifetime broadening is expected to be more prominent lower in the band (higher binding energy) and small near the Fermi level. The broadening of the individual states is usually assumed[24,25] to be proportional to the square of the binding energy. On the other hand, the matrix element (photoexcitation cross-section) modulates the photoelectron intensity in *d*-band metals by a factor usually assumed to be of the form $(1 + \lambda E)^{-1}$ where E is the binding energy measured with respect to the center of the *d*-band (located at 1eV for Fe) and λ is an adjustable parameter[22,23].

These two effects have been included in Figure 7 where a good visual fit was obtained by energy-broadening the individual states of the Moruzzi et al[13] DOS using a broadening function having the form $\Delta E \; \alpha \; 0.9 \; E_B$. The close fit obtained supports the necessity of adding the above two effects when comparing the theoretical DOS with experiment. The same broadening function is used below when comparing the high temperature Fe valence band measurements to the various DOS calculations for Fe above T_c.

3.2 ELEVATED TEMPERATURES

Figures 8-10 are for the measured valence band at elevated temperatures. Tables I–IV contain calculated parameters from these curves. The variation in data dispersion between figures is due to two factors: 1) transmission variation with slit size and 2) the need to acquire the data before there was substantial surface segregation of S. Table III represents data acquired by ramping the sample temperature as quickly as possible with data taken in narrow binding energy windows for the background and the valence band intensity maximum.

Count totals in the tables are presented for those cases in which the number of passes at each temperature were the same, otherwise count rates are given. Note, for example in Figure 10, that although the count rates are similar, the number of passes was very different, as evidenced by the difference in data dispersion.

Examination of Figures 8-10 shows that there is probably a negligible difference (with respect to relative intensity and shape) between the fast-temperature ramp spectra of Figures 9 and 10 and the slow-ramp improved-statistics data of Figure 8. A discussion of difference spectra based on Figure 8 and the combined 1.034 T_c data of Figure 9 and 10 was presented previously[26], the conclusions of which are the following:

1) the intensity remains relatively constant ("invariant points") with temperature at binding energies where the spin polarization of Fe is zero at room temperature;

2) temperature-induced shifts observed in the spectra near E_F can be attributed to the temperature-smearing of the Fermi distribution function and;

3) the high-temperature valence band XPS data presented above disagrees with any of the predicted DOS's for Fe above T_c.

A comparison of the high temperature DOS's with the data was done in Figure 3 of reference 26 without the broadening introduced in Figure 7 of this

paper. Figures 11-14 show the results of that broadening for the theoretical DOS's discussed in reference 26. The relative intensity scale was determined for each of the theoretical DOS's by comparing each with the calculation of Moruzzi et al[3] used in Figure 2. The instrument resolution used for convolution in Figures 11-14 included a FWHM of 1.0eV reflecting the use of 4mm slits in the experimental data of Figure 8. The matrix-element correction and lifetime broadening function used was the same as that of Figure 7. The experimental data used in Figures 11-14 is the T=0.964 T_c curve of Figure 8 (because of its better statistics).

Figure 14 shows the T=0 DOS of Moruzzi et al[3] calculated in Figure 7 for comparison purposes. Figures 11-13 predict a decrease of about 30% in the major peak around 1eV binding energy. In addition, there is a strong change in the DOS shape predicted for each of the high temperature DOS's. Clearly, the data shows that there is little change in the valence band measurement between room temperature and T_c.

4. Summary

We have measured the XPS valence band of Fe(100) at both room temperature and up to temperatures exceeding the Curie temperature, T_c. Good agreement between theory and the room temperature data can be obtained by convolving the ferromagnetic DOS of Moruzzi et al[3] with the instrument resolution, broadening the individual DOS states (with hole lifetime broadening and photoexcitation cross-section modulation) and adding an appropriate inelastic electron (Shirley) background[19] to the result. This procedure is in agreement with the results of others[22–25].

The results at elevated temperatures are different. The observed change in the measured valence band is much less than predicted[1,2,5], even with the aforementioned broadening effects included in the theoretical $T>T_c$ DOS's.

5. References

1. T. Oguchi, K. Terakura and N. Hamada, J. Phys. F 13, 145 (1983).
2. A. J. Pindor, J. Staunton, G.M. Stocks and H. Winter, J. Phys. F 13, 979 (1983).
3. V.C. Moruzzi, J.F. Janak and A.R. Williams, *Calculated Electronic Properties of Metals*, Pergamon, N.Y. (1978).
4. E.P. Wohlfahrt, Rev. Mod. Phys. 25, 211 (1953).
5. T. Jarlborg and M. Peter, J. Magnetism and Mag. Mat. 42, 89 (1984).
6. V. Korenman, J. Murray and R.E. Prange, Phys. Rev. B16, 4032 (1977).
7. M.V. You and V. Heine, J. Phys. F 12, 177 (1982).
8. A.M. Turner and J.L. Erskine, Phys. Rev. B25, 1983 (1982).
9. E. Kisker, K. Schröder, M. Campagna and W. Gudat, Phys. Rev. Lett. 52, 2285 (1984).
10. C.S. Fadley and D.A. Shirley, Phys. Rev. A2, 1109 (1970).
11. C.S. Fadley and D.A. Shirley, Phys. Rev. Lett.21, 980(1968).
12. H. Höchst, P. Steiner and S. Hüfner, Z. Phys. B30, 145 (1978).
13. P.J. Feibelmann and D.E. Eastman, Phys. Rev. B10, 4932 (1974).
14. N.J. Shevchik, Phys. Rev. B16, 3428 (1977).
15. L.C. Davis, N.C. MacDonald, P.W. Palmberg, G.E. Riach and R.E. Weber, *Handbook of Auger Electron Spectoscopy*, Physical Electronics Ind., 2nd ed., (1976).
16. *International Mathematical and Statistical Libraries, Inc., Houston, Texas.*
17. C.H. Reinsch, Numerische Mathematik 10, 177 (1967).
18. C. de Boor, *A Practical Guide To Splines, Applied Mathematical Sciences Series*, Vol. 27, Springer-Verlag, N.Y.(1978).

19. D.A. Shirley, Phys. Rev. B5, 4709 (1972).

20. S. Ohnishi, A.J. Freeman and M. Weinert, Phys. Rev. B28, 6741 (1983).

21. M.P. Seah and W.A. Dench, Surface Inter. Anal. 1, 2(1979).

22. H. Höchst, S. Hüfner and A. Goldmann, Physics Letters 57A, 265(1976) (Fe, Co, Pd, Pt).

23. H. Höchst, S. Hüfner and A. Goldmann, Solid State Comm. 19, 899(1976) (Nb_3Sn, Nb, Sn).

24. P. Steiner, H. Höchst, J. Schneider, S. Hüfner and C. Politis, Z. Physik B33, 241(1979) (Hf, $HfC_xN_yO_z$ compounds).

25. T. Jarlborg and P.O. Nilsson, J. Phys. C 12, 265 (1979) (A15 compounds).

26. R.E. Kirby, E. Kisker, F.K. King and E.L. Garwin, SLAC-PUB-3576.

TABLE I

Maximum of the smoothed XPS Fe valence band peak
as a function of temperature, single run, multi-pass, 4mm slits,
0.114eV steps, 10sec/point total accumulation time.
Data from Figure 8.

Temperature	V.B. Peak Height (counts)	V.B. FWHM (eV)
.283 T_c	926 ±37.3	4.06
.860 T_c	876 ±36.5	4.20
.931 T_c	943 ±37.6	4.25
.964 T_c	943 ±37.6	4.16

TABLE II

Similar conditions as for Table I, single run, multi-pass, 2mm slits,
0.100eV steps, 4 sec/point total accumulation time.
Data from Figure 9.

Temperature	V.B. Peak Height (counts)	V.B. FWHM (eV)
.283 T_c	89 ±11.5	3.68
.808 T_c	97 ±11.6	4.17
.904 T_c	98 ±11.4	4.88
1.002 T_c	104 ±11.6	5.13
1.034 T_c	101 ±12.0	4.80

TABLE III

Maximum of the smoothed XPS Fe valence band peak
during a fast temperature ramp of 1.36 K sec^{-1},
single run, multi-pass profile, 2mm slits, 0.100eV step.

Temperature Range	**V.B. Peak Height (Count Rate)**
.3–.4 T_c	21.1 ±3.3 Hz (3 sec/point)
.4–.9 T_c	19.3 ±3.6 Hz (2.5 sec/point)
.9–1.01 T_c	22.7 ±3.7 Hz(2.5 sec/point)
1.01–1.03 T_c	21.0 ±2.5 Hz(5 sec/point)

TABLE IV

Similar conditions as for Table I, single run, multi-pass, 2mm slits, 0.100ev step.
Data from Figure 10.

Temperature	**V.B. Peak Height (Count Rate)**	**V.B. FWHM (eV)**
.283 T_c	25.5 ±1.3 Hz (22.5 sec/point)	1.3
1.034 T_c	25.35 ±4.2 Hz (2 sec/point)	4.2

Figure Captions

1. Fe(100), room temperature, XPS survey scan, 2 mm slits. Data (....), spline fit (——).

2. Fe(100) XPS valence band, 2 mm slits. Position of principle features is indicated. Data (....) spline fit (——).

3. Data of Figure 2 (....) with convolution of Moruzzi et al[3] DOS and instrument resolution, Shirley background (——) added. Total fit(——).

4. Data of Figure 2 (....) with convolution of Ohnishi et al[20] DOS (center layers only)and instrument resolution, Shirley background added. Total fit (——).

5. Data of Figure 2 (....) with convolution of Ohnishi et al[20] DOS (1 surface layer, 7 center layers) and instrument resolution, Shirley background added. Total fit(——).

6. Data of Figure 2 (....) with convolution of Ohnishi et al[20] DOS (2 surface layer, 6 center layers) and instrument resolution, Shirley background added. Total fit(——).

7. Data of Figure 2 (....) with convolution of Moruzzi et al[3] DOS and instrument resolution broadened by $\Delta E \ \alpha \ 0.9 \ E_B$, Shirley background added. Total fit (——).

8. Valence band as a function of temperature, 4 mm slits, equal number of passes, single run. Successive curves offset 30 Hz vertically with respect to each other.

9. Same as Figure 8, except 2 mm slits, single run. Successive curves offset 15 Hz vertically with respect to each other.

10. Single run, different number of passes, 2 mm slits. Top curve offset 20 Hz vertically.

11. Data of Figure 8 ($0.964T_c$) scaled for 2mm slits, with convolution of Jarlborg and Peter[5] DOS and 4mm (1.0 eV FWHM) instrument resolution broadened by $\Delta E \ \alpha \ 0.9E_B$, Shirley background added. Total fit(——).

12. Same as Figure 11 except DOS is that of Pindor et al[2]

13. Same as Figure 11 except DOS is that of Oguchi et al[1].

14. Same as Figure 11 except the T=0 DOS of Moruzzi et al[3] is used, for comparison.

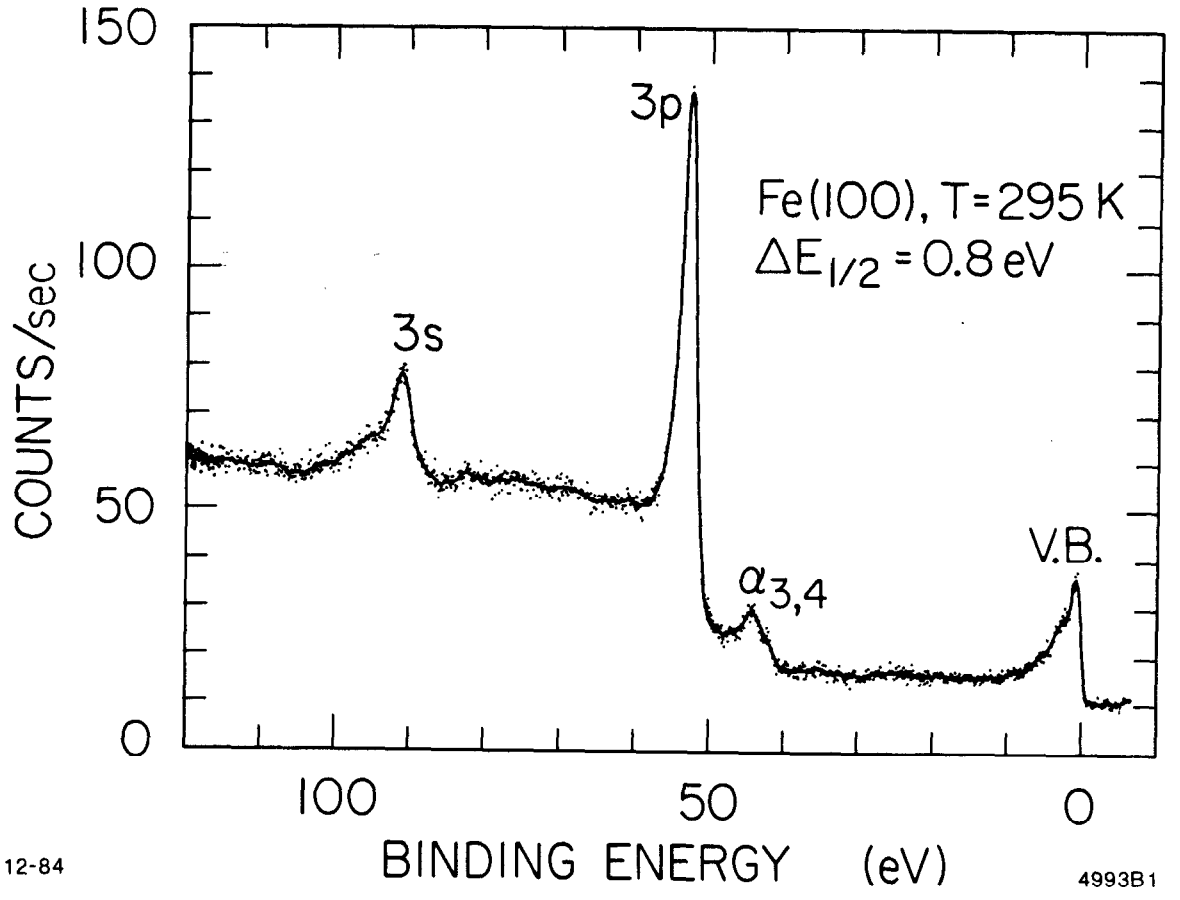
150
100
50
0
COUNTS/sec
3p
3s
$\alpha_{3,4}$
V.B.
Fe(100), T=295 K
$\Delta E_{1/2}$ = 0.8 eV
100
50
0
BINDING ENERGY (eV)
12-84
4993B1

Fig. 1

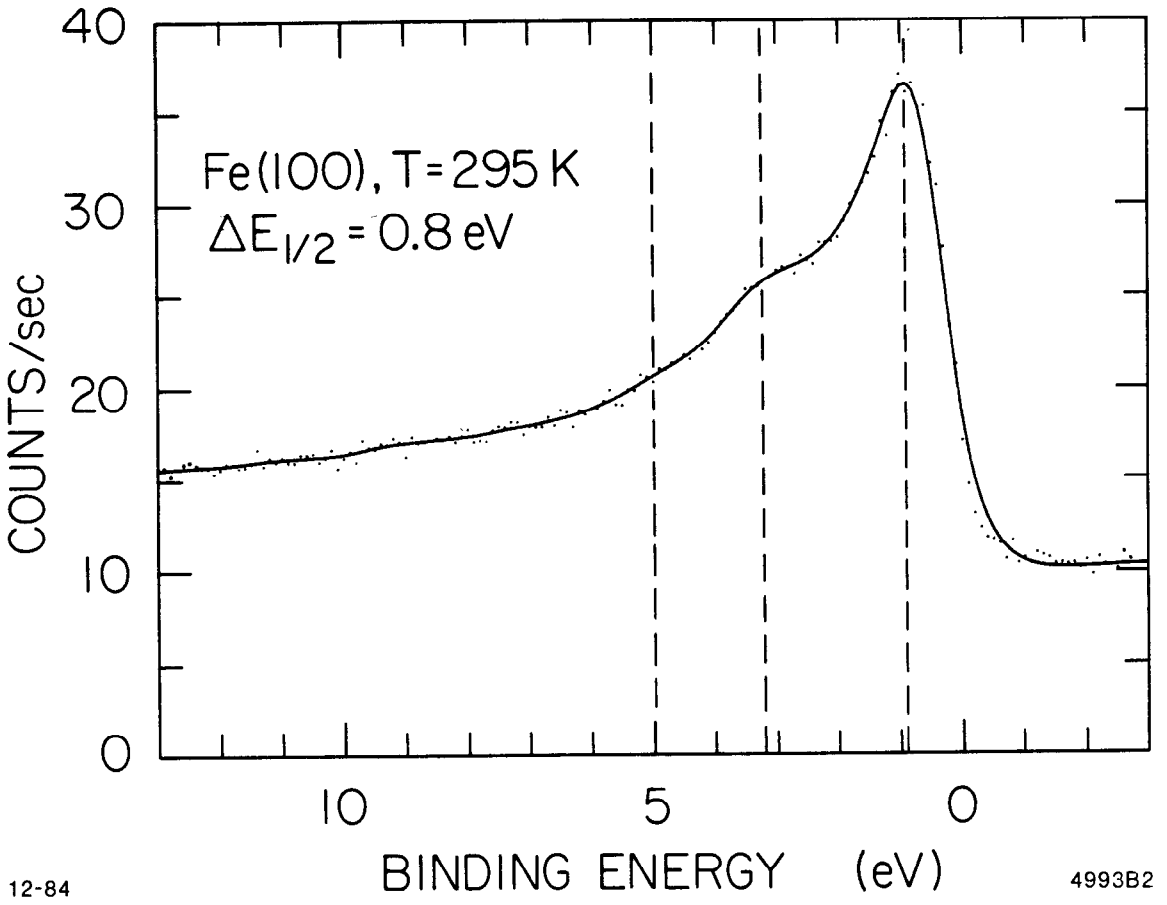
40
30
20
10
0
COUNTS/sec
Fe(100), T=295 K
ΔE1/2 = 0.8 eV
10
5
0
BINDING ENERGY (eV)
12-84
4993B2

Fig. 2

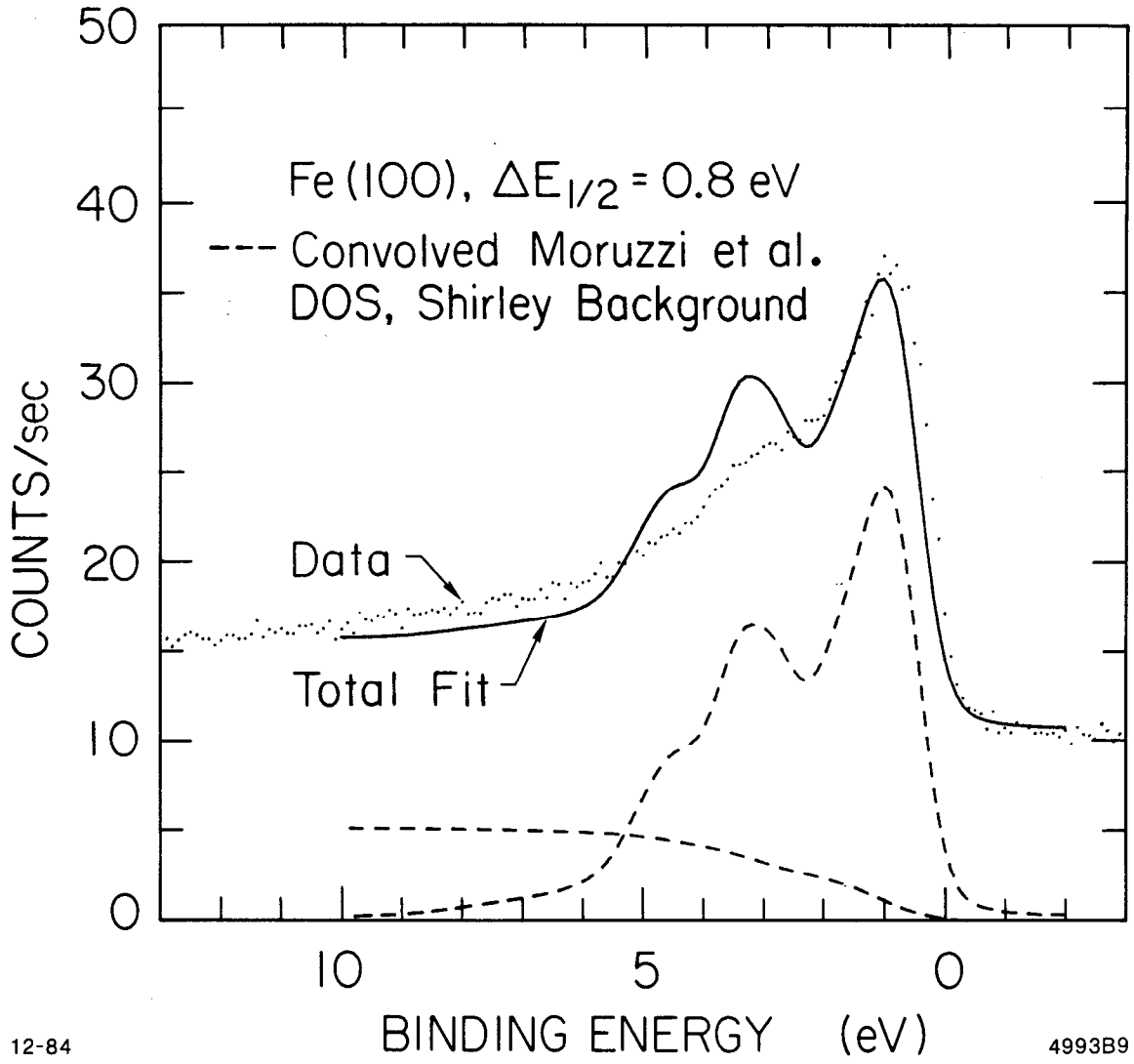
Fe(100), $\Delta E_{1/2}$ = 0.8 eV
Convolved Moruzzi et al. DOS, Shirley Background
Data
Total Fit
COUNTS/sec
BINDING ENERGY (eV)
50
40
30
20
10
0
10
5
0
12-84
4993B9

Fig. 3

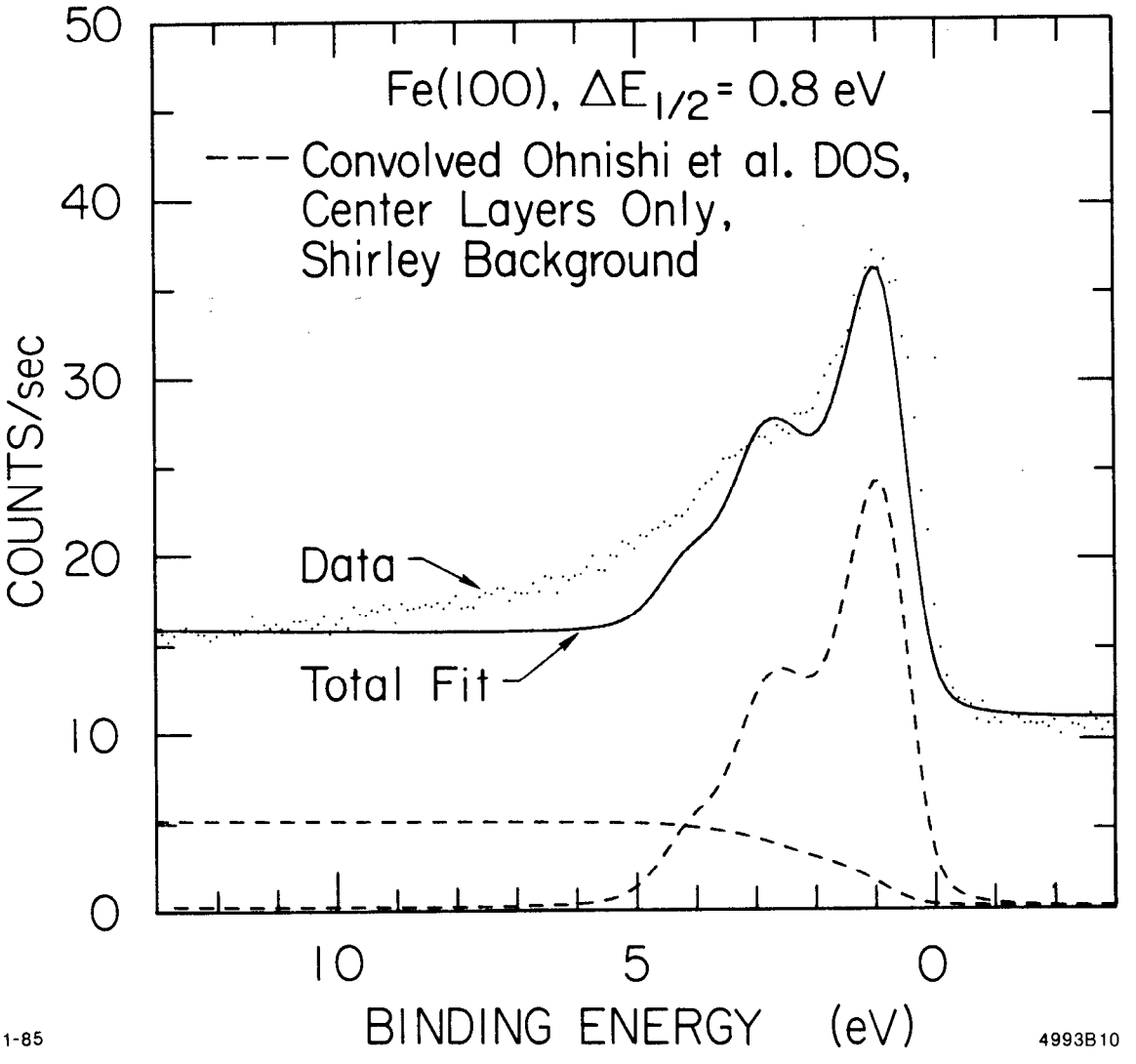
Fe(100), $\Delta E_{1/2}$ = 0.8 eV
Convolved Ohnishi et al. DOS,
Center Layers Only,
Shirley Background
Data
Total Fit
COUNTS/sec
50
40
30
20
10
0
10
5
0
BINDING ENERGY (eV)
1-85
4993B10

Fig. 4

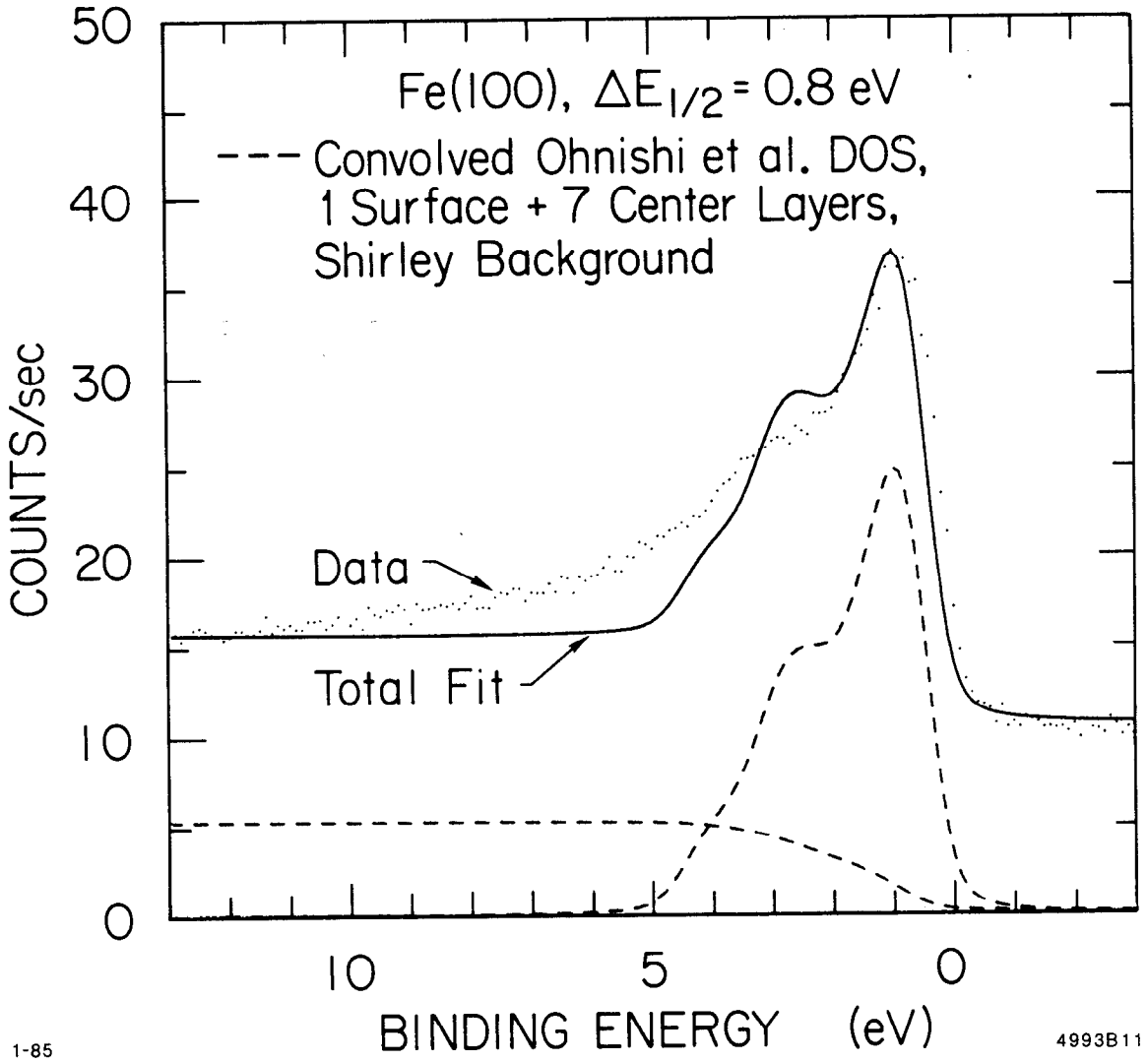
Fe(100), $\Delta E_{1/2}$ = 0.8 eV
Convolved Ohnishi et al. DOS,
1 Surface + 7 Center Layers,
Shirley Background
Data
Total Fit
COUNTS/sec
BINDING ENERGY (eV)
50
40
30
20
10
0
10
5
0
1-85
4993B11

Fig. 5

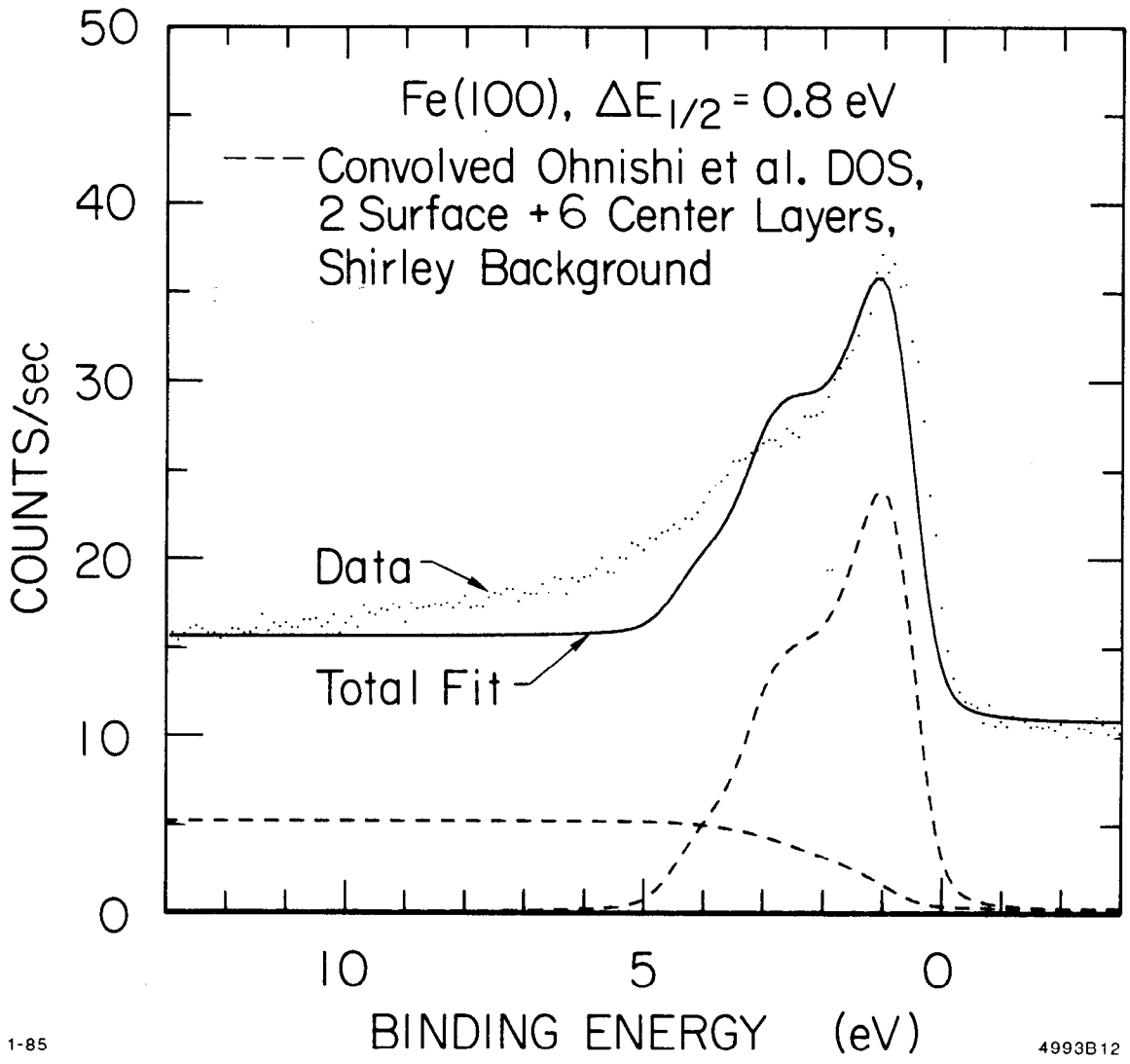
Fe(100), $\Delta E_{1/2}$ = 0.8 eV
Convolved Ohnishi et al. DOS,
2 Surface + 6 Center Layers,
Shirley Background
Data
Total Fit
COUNTS/sec
50
40
30
20
10
0
10
5
0
BINDING ENERGY (eV)
1-85
4993B12

Fig. 6

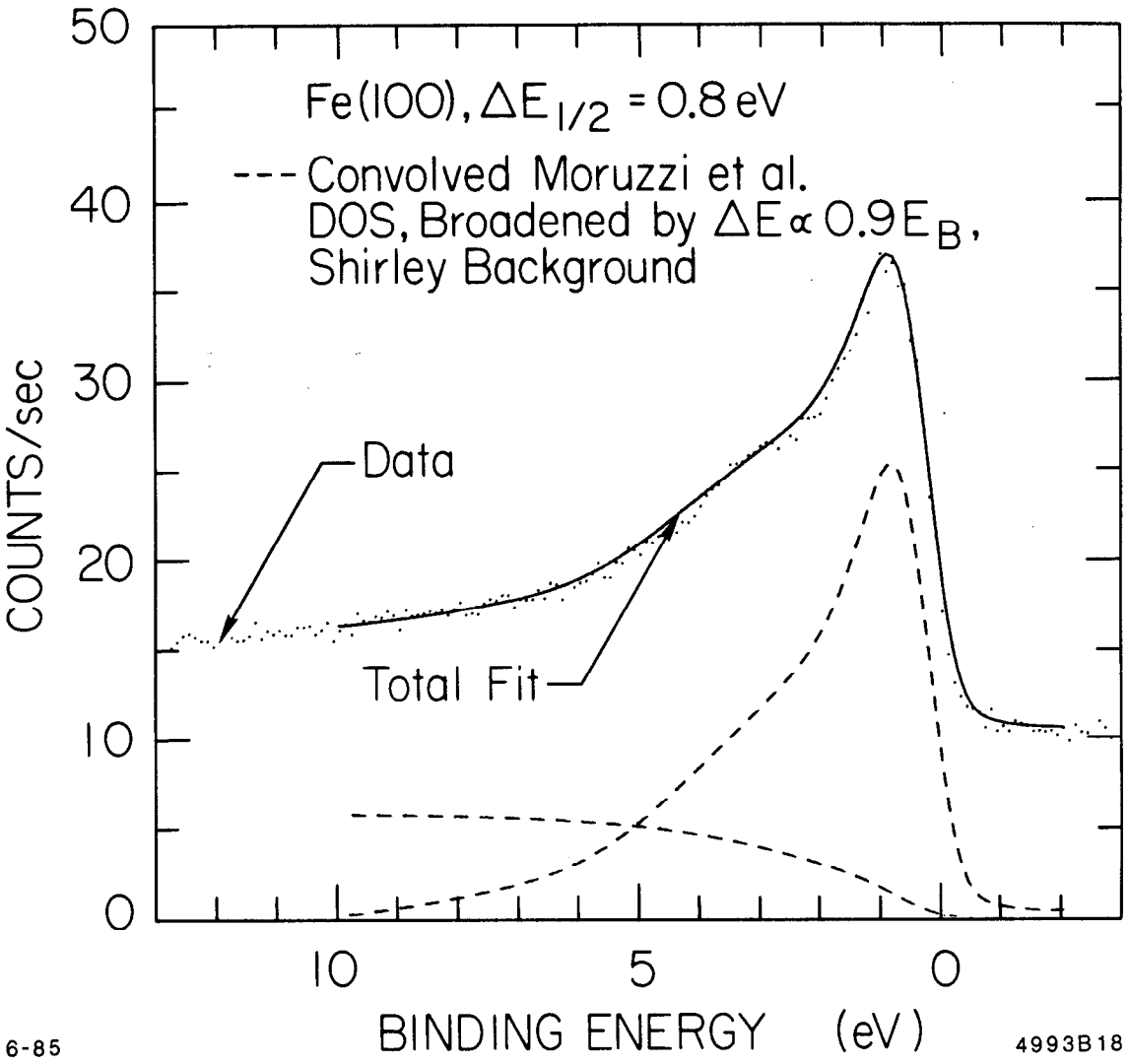
Fe(100), $\Delta E_{1/2}$ = 0.8 eV
--- Convolved Moruzzi et al. DOS, Broadened by $\Delta E \propto 0.9 E_B$, Shirley Background
Data
Total Fit
COUNTS/sec
BINDING ENERGY (eV)
50
40
30
20
10
0
10
5
0
6-85
4993B18

Fig. 7

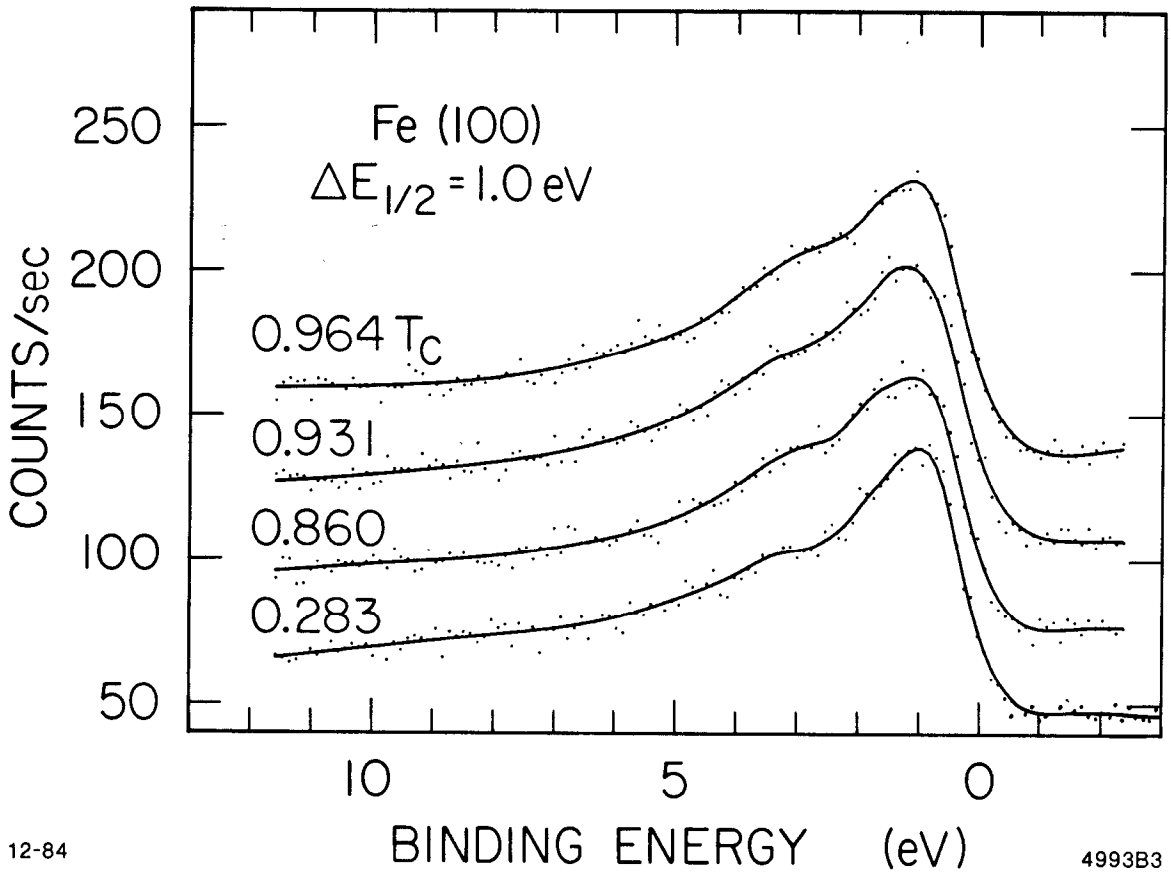
Fe (100)
$\Delta E_{1/2}$ = 1.0 eV
0.964 T_C
0.931
0.860
0.283
250
200
150
100
50
COUNTS/sec
10
5
0
BINDING ENERGY (eV)
12-84
4993B3

Fig. 8

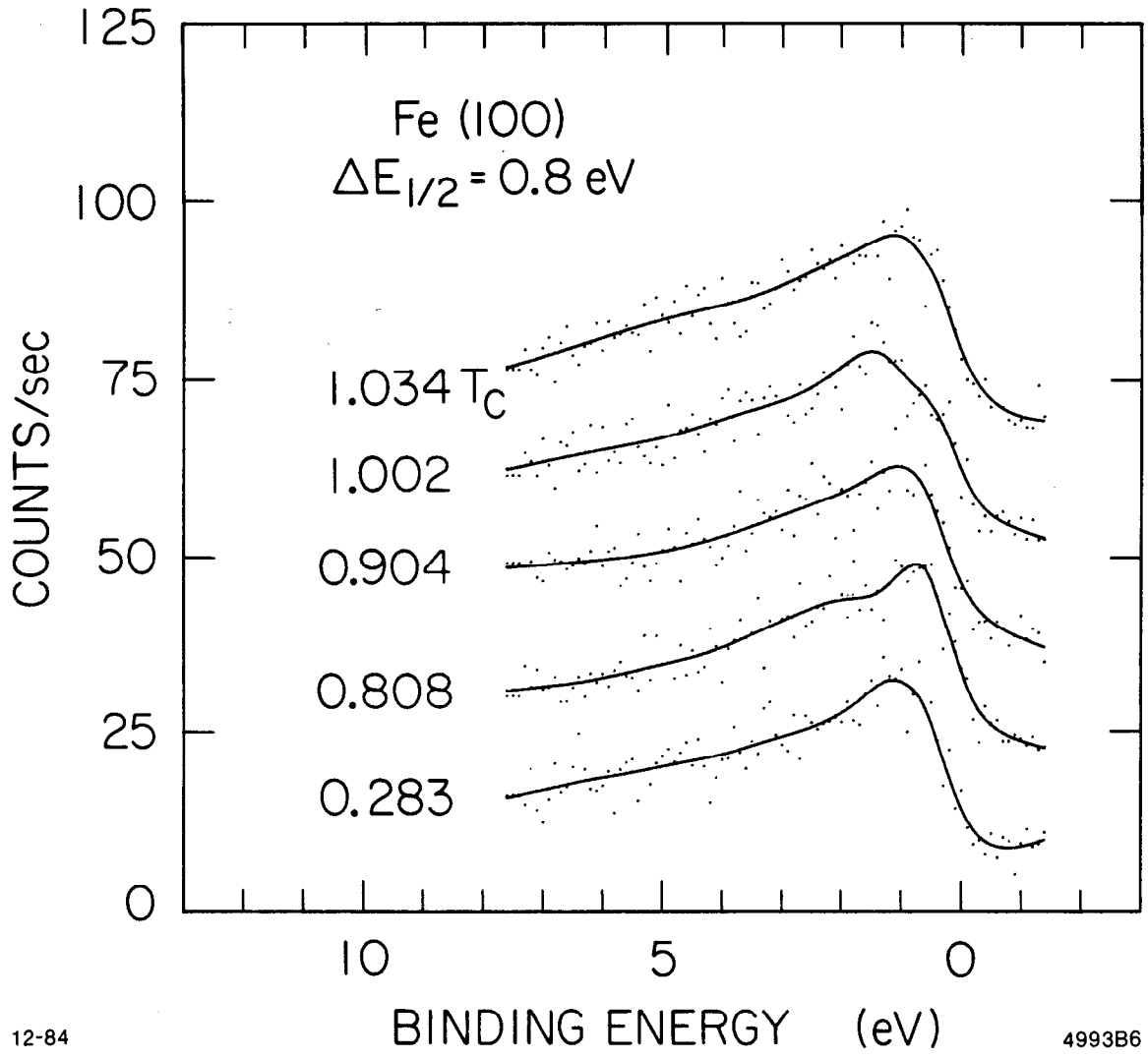
125
100
75
50
25
0
COUNTS/sec
Fe (100)
ΔE1/2 = 0.8 eV
1.034 TC
1.002
0.904
0.808
0.283
10
5
0
BINDING ENERGY (eV)
12-84
4993B6

Fig. 9

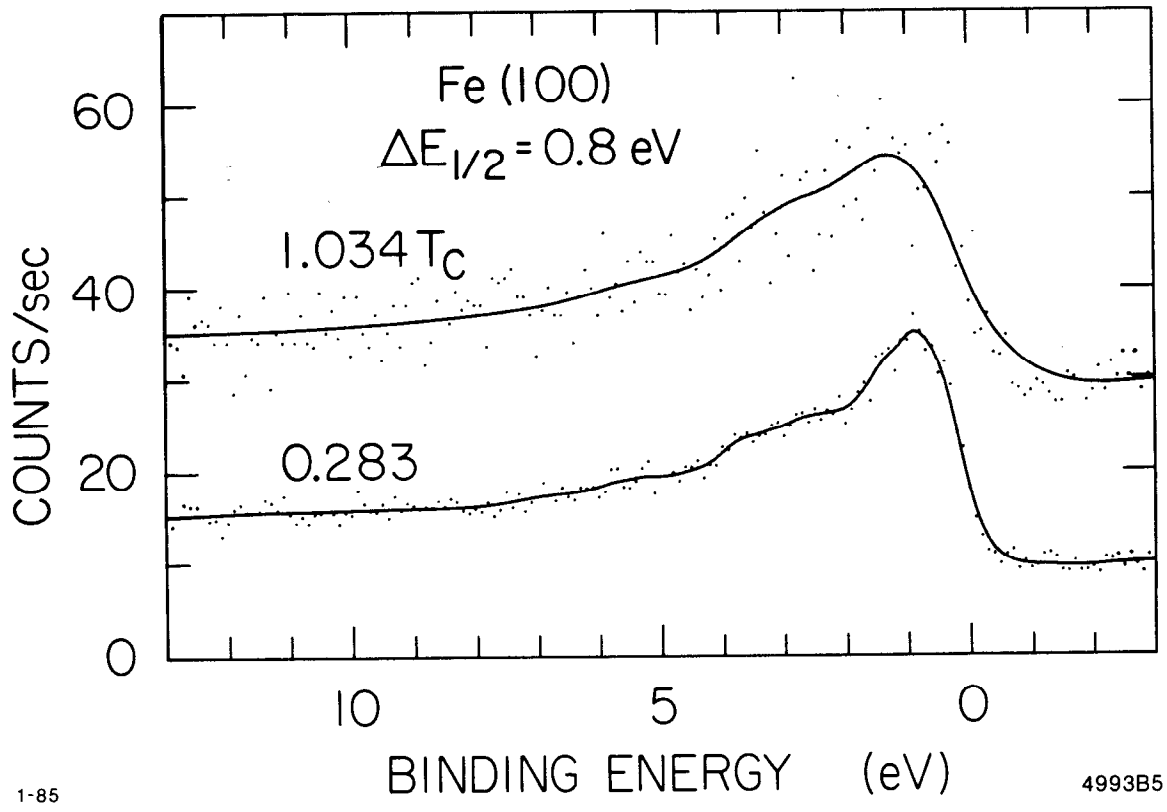
Fe (100)
ΔE1/2 = 0.8 eV
1.034 TC
0.283
60
40
20
0
COUNTS/sec
10
5
0
BINDING ENERGY (eV)
1-85
4993B5

Fig. 10

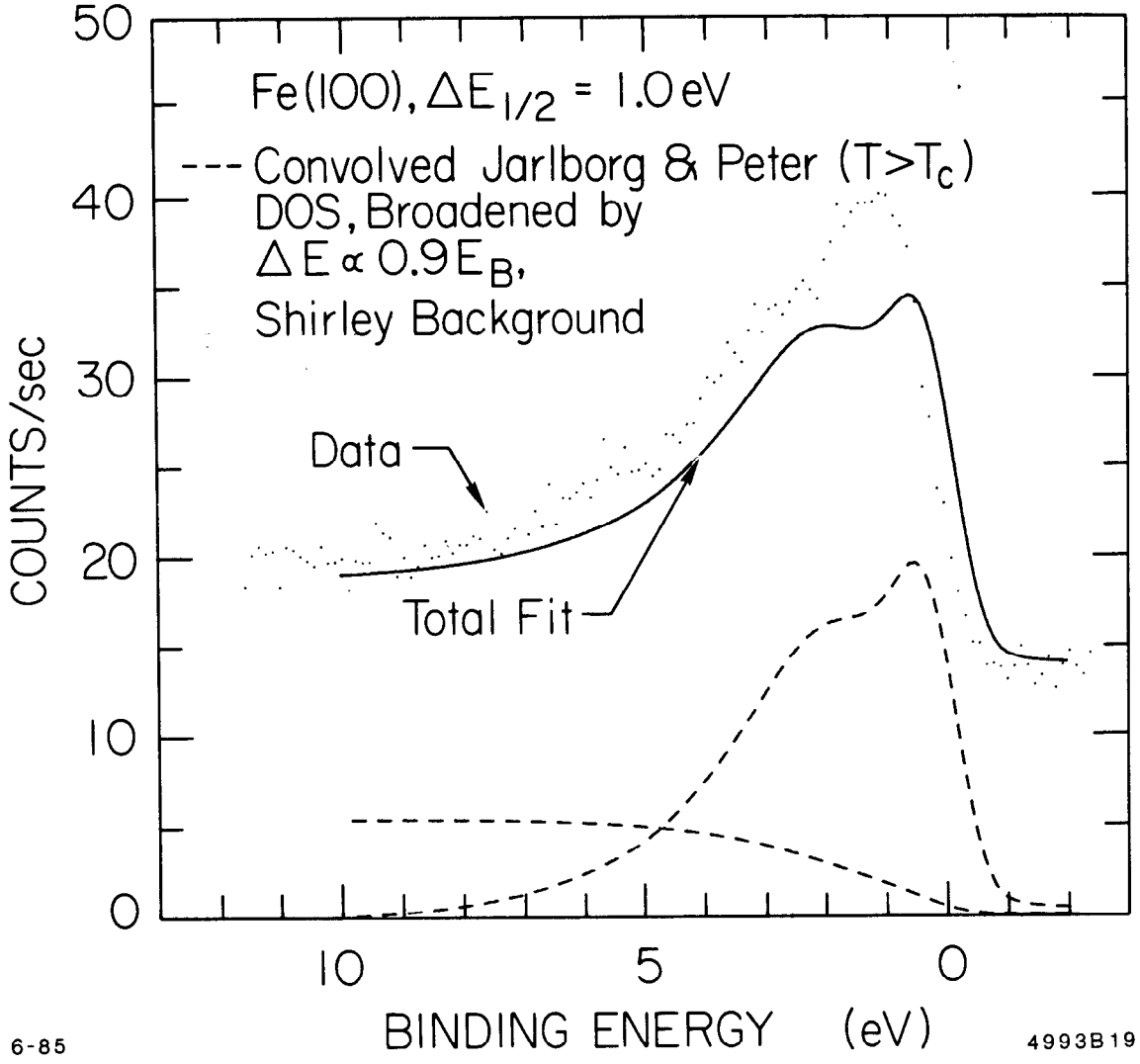
Fe(100), $\Delta E_{1/2}$ = 1.0 eV
--- Convolved Jarlborg & Peter (T>T_c) DOS, Broadened by $\Delta E \propto 0.9 E_B$, Shirley Background
Data
Total Fit
COUNTS/sec
50
40
30
20
10
0
10
5
0
BINDING ENERGY (eV)
6-85
4993B19

Fig. 11

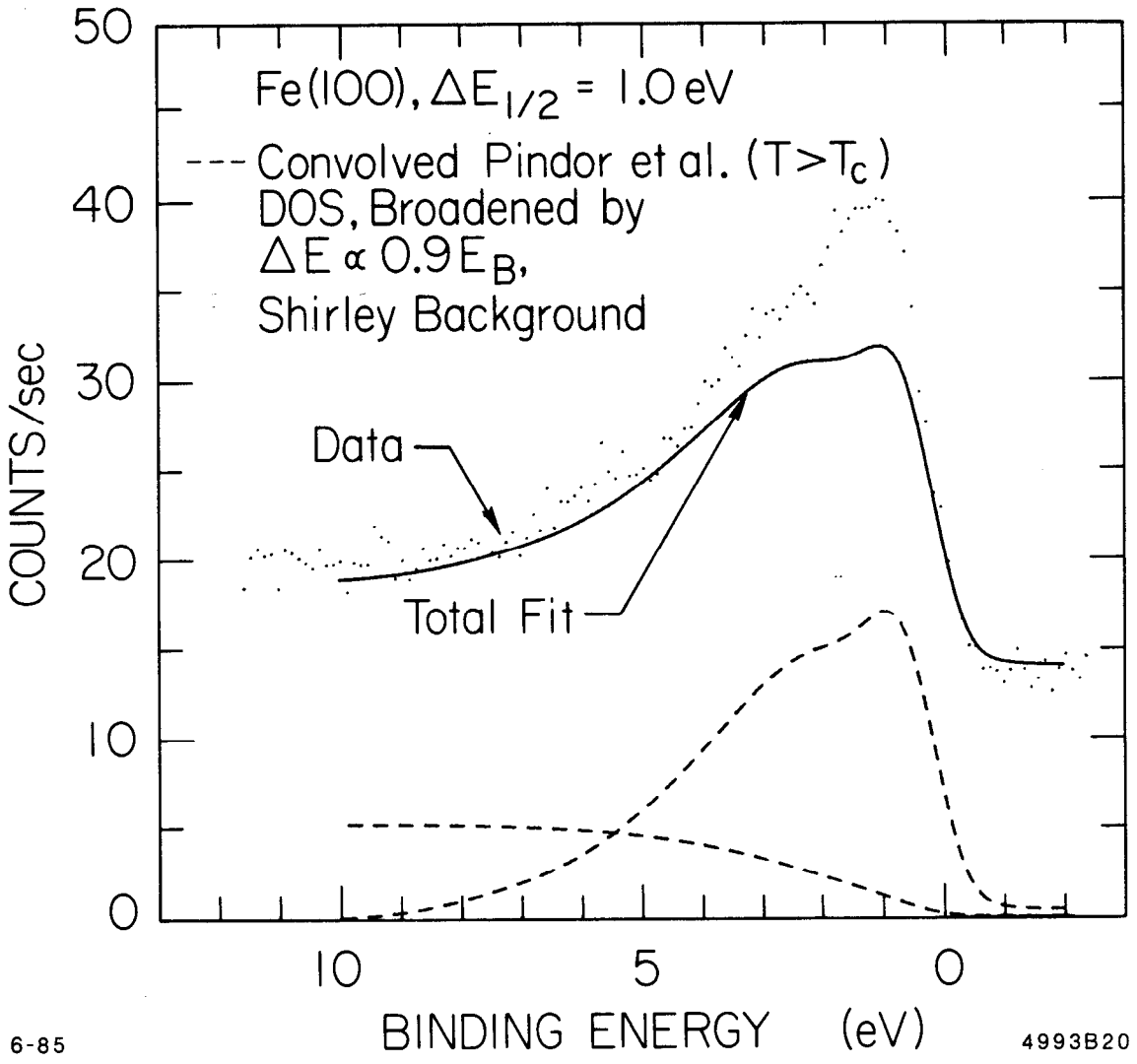
Fe(100), $\Delta E_{1/2}$ = 1.0 eV
--- Convolved Pindor et al. (T>T_c)
DOS, Broadened by
$\Delta E \propto 0.9 E_B$,
Shirley Background
Data
Total Fit
COUNTS/sec
50
40
30
20
10
0
10
5
0
BINDING ENERGY (eV)
6-85
4993B20

Fig. 12

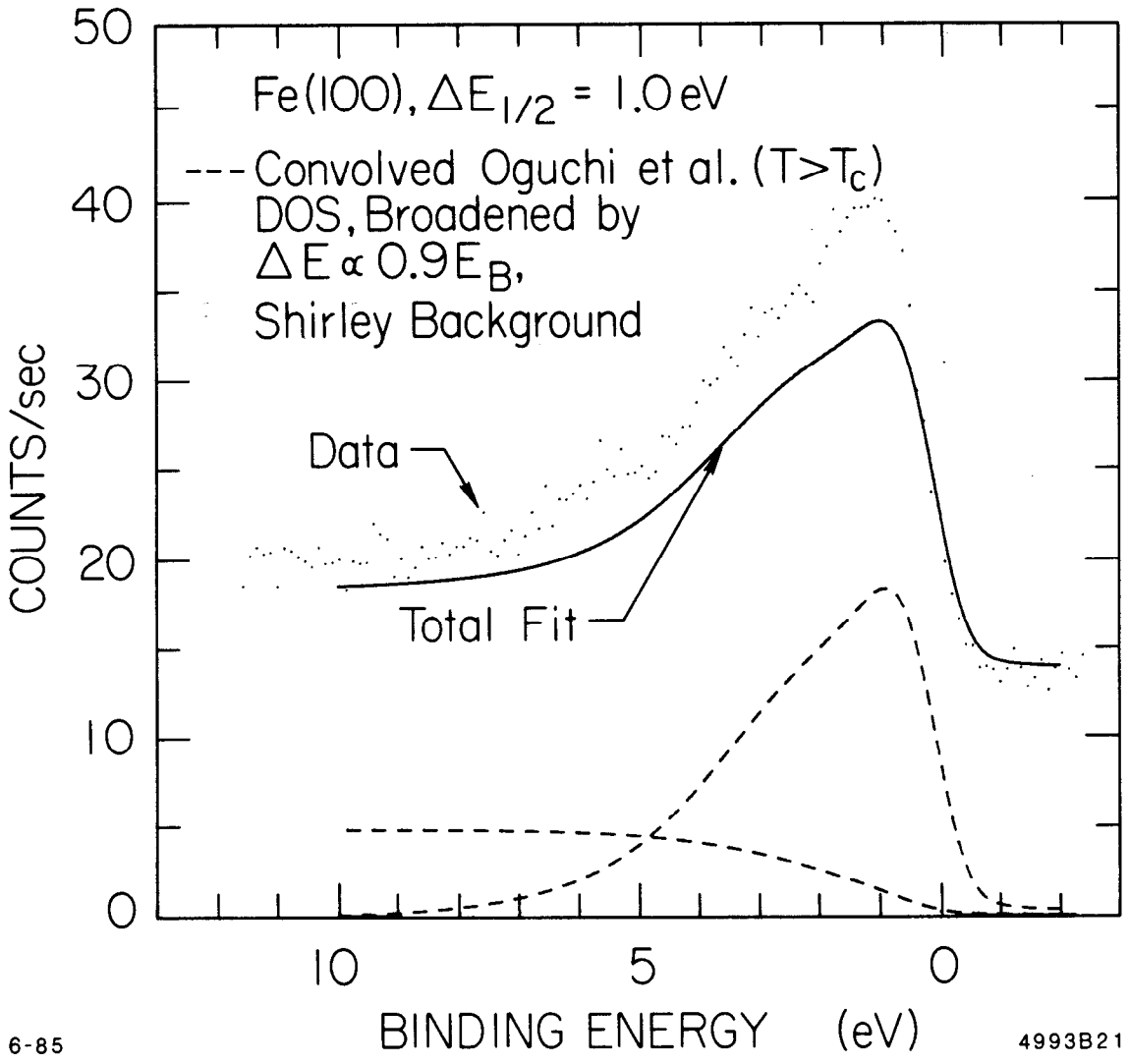
Fe(100), $\Delta E_{1/2}$ = 1.0 eV
--- Convolved Oguchi et al. (T>T_c) DOS, Broadened by $\Delta E \propto 0.9 E_B$, Shirley Background
Data
Total Fit
COUNTS/sec
50
40
30
20
10
0
10
5
0
BINDING ENERGY (eV)
6-85
4993B21

Fig. 13

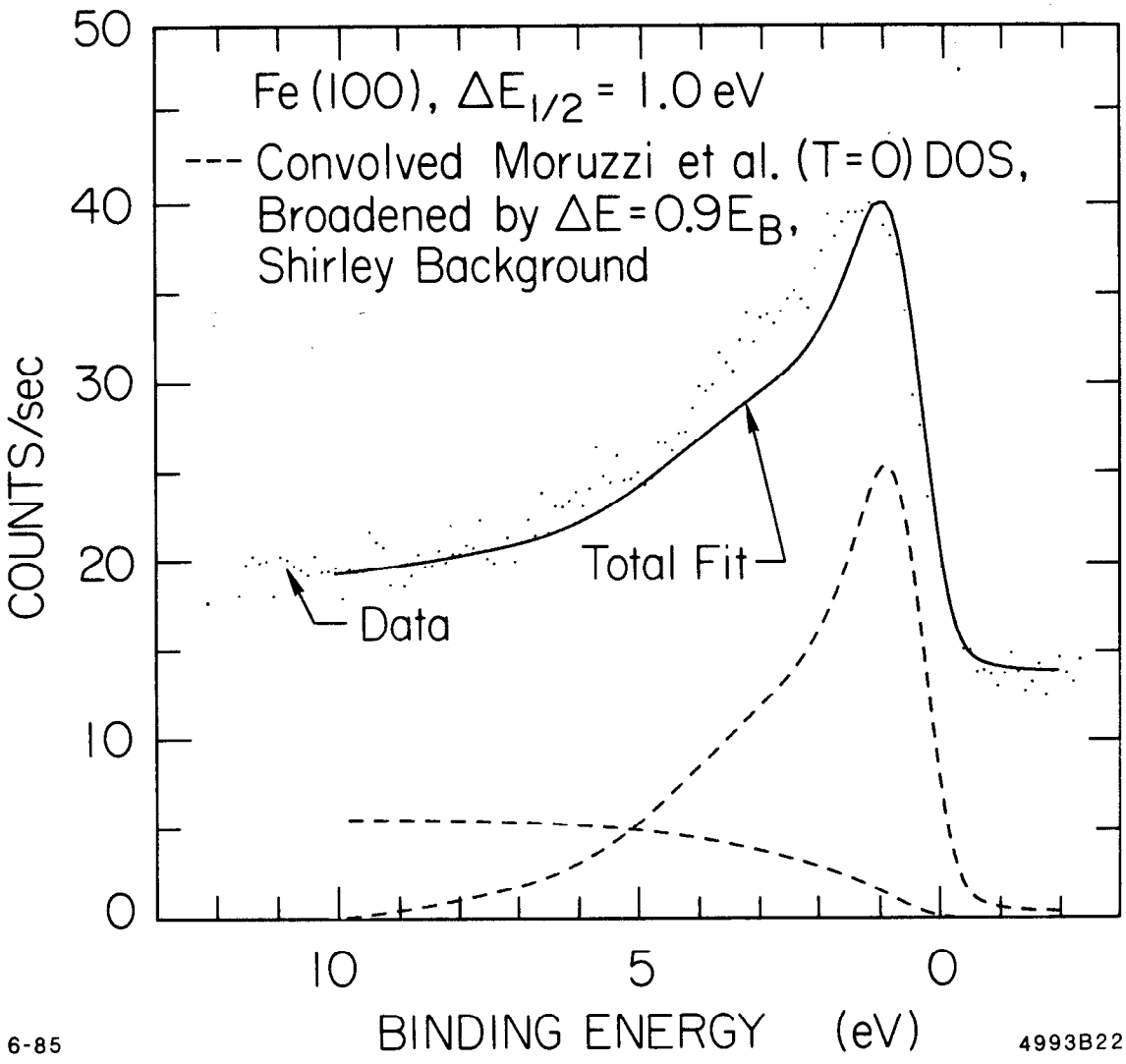
Fe (100), $\Delta E_{1/2}$ = 1.0 eV
--- Convolved Moruzzi et al. (T=0) DOS,
Broadened by $\Delta E = 0.9E_B$,
Shirley Background
Total Fit
Data
COUNTS/sec
50
40
30
20
10
0
10
5
0
BINDING ENERGY (eV)
6-85
4993B22

Fig. 14